

**Traffic flow in a crowd of pedestrians walking at different speeds**Akihiro Fujita,<sup>1,\*</sup> Claudio Feliciani,<sup>2</sup> Daichi Yanagisawa,<sup>2</sup> and Katsuhiro Nishinari<sup>2</sup><sup>1</sup>*Department of Aeronautics and Astronautics, School of Engineering, The University of Tokyo, 7-3-1, Hongo, Bunkyo-ku, Tokyo 113-8656, Japan*<sup>2</sup>*Research Center for Advanced Science and Technology, The University of Tokyo, 4-6-1, Komaba, Meguro-ku, Tokyo 153-8904, Japan*

(Received 9 January 2019; published 17 June 2019)

This study investigates motion in a crowd of pedestrians walking at different speeds. Three pedestrian groups are considered (slow walkers, normal walkers, and fast walkers), and we design the experimental condition by mixing the normal walkers with either the slow or the fast walkers to create flows with different speed compositions. All the walkers in this experiment were instructed to walk along a circular course unidirectionally. Fundamental diagrams and multiple regression analysis show that the speed at which a particular pedestrian walks is determined by both the local density and the speed at which the surrounding pedestrians are walking. We also find that the spontaneous lane formation, that occurs in bidirectional flow, does not occur in flow in which the speed is heterogeneous, thereby resulting in a spatial density distribution with large variance. This corresponds to pedestrian clustering, which reduces both the mean speed and the flow rate.

DOI: [10.1103/PhysRevE.99.062307](https://doi.org/10.1103/PhysRevE.99.062307)**I. INTRODUCTION**

With a rapidly growing global population, excessively large crowds and congestion have become serious problems in both developed and developing countries. To mitigate this, numerous studies have been conducted to understand the behavior of pedestrian crowds and their evacuation processes [1–3]. In such studies, the fundamental diagrams, which show the relationship between speed and density, were used widely for validation of simulation models [4,5]; however, it was also found that the crowd movements are affected greatly by factors such as facility geometry [6,7], the rhythms that pedestrians hear [8], and cultural differences [9,10]. Therefore, it is necessary to understand these other factors that influence crowd movement.

Among these factors, age is attracting much interest because of the aging population in several countries. Investigations in the form of simulations, observations, and experiments have considered how age difference affects the flow characteristics. In this field, simulation models that consider behavioral differences among individuals have been built [11]. Observational studies on pedestrians with different age compositions were conducted [12,13], and controlled experimental studies that consider age difference have been conducted widely. The subjects of these studies included small children [14,15], people who were older or less fit [16], and people with disabilities [17–19]. However, these experimental studies focused mainly on groups of one type of pedestrian (i.e., groups comprising only children, older adults, or people with disabilities), and mixed situations (i.e., groups comprising different types of pedestrians walking simultaneously) were rarely considered. One study that did focus on age differences in mixed situations concluded that heterogeneous flow is

more likely to cause jams because of pedestrian interactions [20]. However, that study allowed space for only one lane of pedestrian traffic, thereby permitting only one-dimensional movement and limiting the knowledge obtained from the study.

Even though previous research has focused on age difference, that aspect encompasses several physical heterogeneities such as differences in walking speed, motivation, and reaction time. Therefore, it is difficult to obtain a generalized idea on what physical quantity affects the flow characteristics if we focus on age heterogeneity alone.

Accordingly, in the present study, we focus on speed differences among pedestrians and investigate how they influence the walking speed of an individual pedestrian and the macroscopic behavior of the flow such as mean speed and density distribution. To understand the effect of speed difference and to study two-dimensional movements (thereby expanding on previous results), we conducted experiments using the circular course shown in Fig. 1.

The remainder of this paper is organized as follows. In Sec. II, we describe the experimental setup. In Sec. III, we present the difference in fundamental diagrams and analyze how the speed at which an individual pedestrian walking affects the speed at which an individual pedestrian walks. In Sec. IV, we present the macroscopic flow characteristics. Finally, in Sec. V, we summarize and discuss the conclusion of the study.

**II. EXPERIMENT SETUP**

The goal of our experiments was to elucidate how speed heterogeneity influences individual pedestrians and the flow characteristics. The experiments were conducted in 2017 at the University of Tokyo, Japan. Figure 1 shows a snapshot of an experiment, all of which were conducted in a ring-shaped corridor, and a sketch of the experimental field, the inner and

\*f-akihiro@g.ecc.u-tokyo.ac.jp

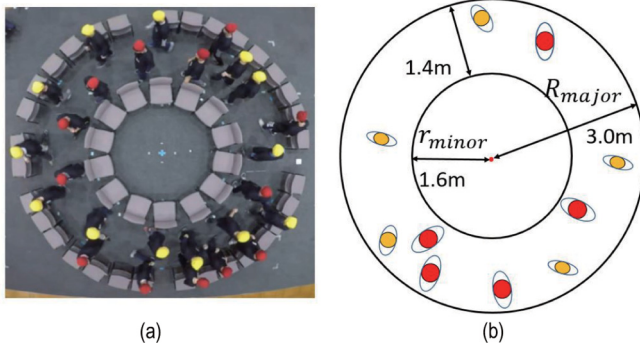


FIG. 1. (a) Snapshot of the experiment. (b) Experimental field.

outer radii of which were set to 1.6 and 3.0 m, respectively. The width of the corridor was thus 1.4 m, and the area of the experimental field was approximately 20.0 m<sup>2</sup>. This course was sufficiently wide for two-dimensional behavior to occur. We recruited 32 students as participants, all of whom were male university students aged 18–25 years who applied voluntarily for the experiment and were rewarded financially.

Because the aim of the experiments was to investigate the effects of velocity heterogeneity, crowds with different speed composition were investigated, as shown in Table I. In the case of the slow-mix composition, for example, the participants were divided into two groups: slow walkers and normal walkers. The slow walkers were instructed to walk slower than their normal walking speed (the slower speed was measured as  $0.49 \pm 0.12$  m/s), whereas the normal walkers were instructed to walk at their normal speed and maintain that speed. In addition, the normal walkers were allowed to pass the slow walkers to maintain their walking speed ( $1.07 \pm 0.09$  m/s), thereby making the experimental conditions resemble those of an actual walkway. Similarly, in the case of the fast-mix composition, the fast walkers were asked to walk faster than their normal speed (the faster speed was measured as  $1.71 \pm 0.2$  m/s), whereas the normal walkers were asked to walk normally as before. In this case, the faster walkers were allowed to pass the normal walkers. We performed several test trials in which the participants were instructed to walk at these three different speeds (normal, fast, and slow), and the methods for measuring their desired speeds are written in the Appendix. Note that these desired speeds were measured under low-density conditions (also see Appendix).

The participants wore caps whose color indicated the walking speed, as shown in Fig. 1(a). Normal walkers wore yellow caps, whereas fast and slow walkers wore red caps. In both the slow mix and the fast mix, there were equal numbers of red-cap and yellow-cap participants. We also conducted experiments with homogeneous crowds for reference.

The global density (i.e., the mean density of the entire experimental field) was varied from 0.1 to 1.5 m<sup>-2</sup> in increments of 0.2 m<sup>-2</sup> by changing the number of walkers.

Because of these eight levels of global density and the five as types of composition (Table I), there were  $8 \times 5 = 40$  conditions in total.

In each trial, we instructed the participants when to start and stop, the trial being designed to last for 60 s. We recorded the entirety of each experiment using a video camera mounted

TABLE I. Five crowd compositions.

Composition	Mixed elements
Fast mix	Fast and normal
Slow mix	Slow and normal
Fast (homogeneous)	Fast walkers only
Normal (homogeneous)	Normal walkers only
Slow (homogeneous)	Slow walkers only

on the 6-m-high ceiling of the experiment room, and we used *PeTrack* to extract the participant trajectories which are openly available for download at [21].

### III. EFFECT OF SURROUNDING VELOCITY

#### A. Fundamental diagram

To analyze this experiment, we prepared fundamental diagrams in which we plot flow and speed against local density. In the present study, the speed is calculated as

$$v_t = \frac{|\mathbf{x}_{t+5} - \mathbf{x}_{t-5}|}{10\delta t}. \quad (1)$$

The  $\delta t$  is the frame interval of the data (1/30 s) and  $\mathbf{x}_t$  is the location of each walker at time step  $t$ . Note that  $\mathbf{x}_t$  is a vector and  $v_t$  is a scalar value. This calculation works as a filter to smooth sharp fluctuations in speed. We calculate local density on the basis of the Voronoi method, as presented in [6].

All the plots in Fig. 2 show the speed and density for normal walkers, wherein the color represents the compositions of the crowd. From Fig. 2(a), we see that all the plots are in the free-flow region in which the flow increases with local density. In other words, no congested flow was observed in those experiments even when at the maximum global density of 1.5 m<sup>-2</sup>.

Contrary to previous research, Fig. 2(b) implies that individual walking speed cannot be determined from the local density alone, especially in a crowd with different speeds. Therefore, to study the effect of the surroundings in more detail, in Fig. 2(c) we plot the average speed of the normal walkers for each composition and also the variance of that speed.

The average speed of normal walkers grouped with fast walkers is clearly always higher than that of normal walkers in homogeneous flow. Furthermore, the speed of normal walkers in homogeneous flow is almost always higher than that of normal walkers in the slow-mix composition. In the inset of Fig. 2(c), we plot the effect size (Cohen's  $d$ ) of the  $t$  test conducted to determine if the speed gap has a significant difference. Cohen's  $d$  is calculated for each local density. The gray dotted line represents the significance level, which is set to 0.5 in this analysis. This shows that the velocity is significantly different when the local density is from 0.6 to 2.4 m<sup>-2</sup> in the slow-mix runs and from 1.2 to 2.6 m<sup>-2</sup> in the fast-mix runs. Therefore, even though each participant tried to walk at his normal speed, his actual walking speed was affected significantly by the speed of those around him.

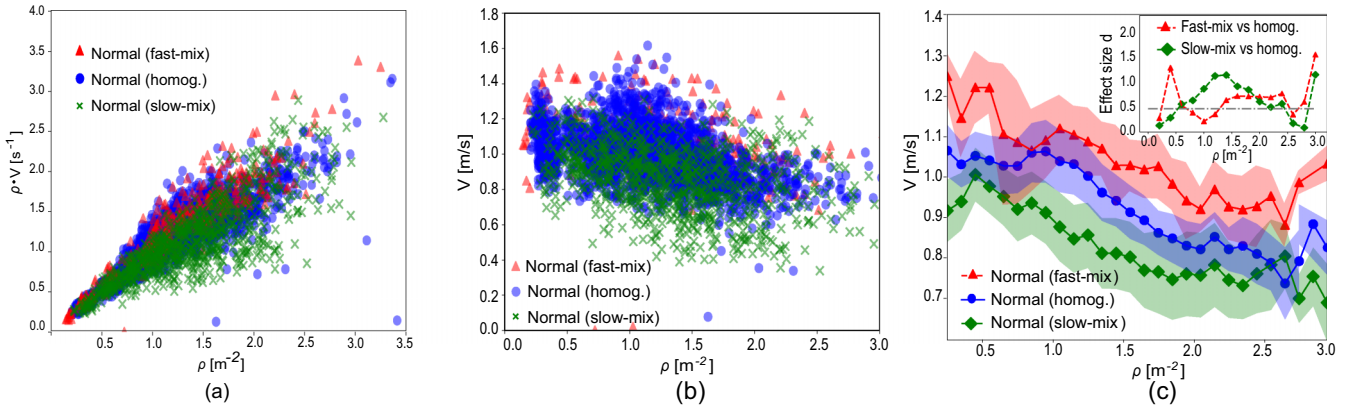


FIG. 2. Fundamental diagrams of normal pedestrians in different compositions: the blue circle represents normal walkers walking with other normal walkers (homogeneous runs), and the red triangle and green diamond represent normal walkers walking with fast and slow walkers, respectively (heterogeneous runs). (a) Flow rate versus density; (b) speed versus density; (c) average speed versus density: the shaded area represents one-sigma error. Inset: the red dotted line with triangles is the result of the  $t$  test between fast-mix and homogeneous flows and the green dotted line with diamonds is that between slow-mix and homogeneous trials.

**B. Surrounding speed**

As mentioned above, the walking speed of the surrounding walkers is clearly an important factor in determining the speed of an individual walker. To examine this observation closely, we introduce a new quantity called “surrounding speed.” This parameter is a value that is assigned to each pedestrian and is calculated as the simple mean of the speeds of other pedestrians who are within a specified range from the given pedestrian [defined as the “region of interest” shown in Fig. 3(a)]. For example, if there are  $n$  pedestrians in the region of interest for a given pedestrian, the surrounding speed of that pedestrian is calculated as

$$v_{\text{sur}} = \frac{1}{n} \sum_i v_i, \tag{2}$$

where  $v_i$  is the speed of the other pedestrian  $i$  (i.e., not the given pedestrian) in the region of interest. The region of interest is shown as the light-blue area in Fig. 3(a) and is

defined as the sector in front of the given pedestrian with a central angle of  $\theta^\circ$ . We chose this sector region because we reasoned that the given pedestrian is not affected by those behind him.

In addition, because in Sec. III C, we conduct multiple-regression analysis, we fix the angle and the region of interest to where the correlation coefficient between local density and surrounding speed is sufficiently small to avoid multicollinearity [22].

The relationship between the correlation coefficient and the central angle is demonstrated in Fig. 3(b). This graph shows that when the local density is too high, the correlation is always too high to investigate the influence of surrounding speed and density separately, regardless of the central angle. It also implies that when the local density is from, the correlation coefficient between  $v_{\text{sur}}$  and  $\rho$  is smaller than 0.2, meaning that these two quantities can be regarded as being independent of each other. Moreover, in that density region, the correlation coefficient is clearly almost independent of the central

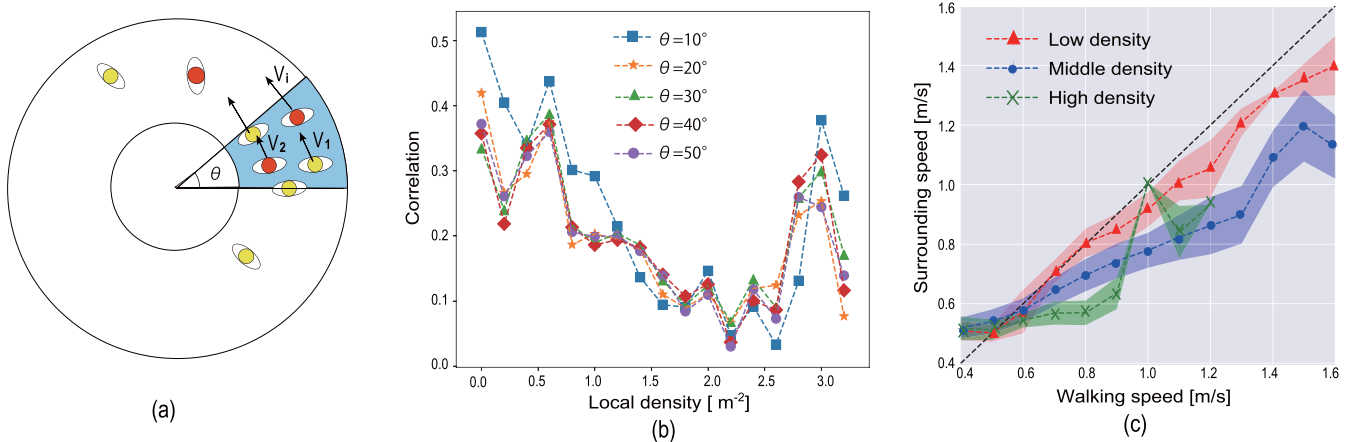


FIG. 3. (a) Region of interest used to define the surrounding speed of a given pedestrian;  $\theta$  is the central angle. (b) Correlation coefficient between local density and surrounding speed versus the local density for different values of central angle as indicated in the legend. (c) Relationship between surrounding speed and walking speed in different density regions: low- ( $\rho \leq 1.0$ ), middle- ( $1.0 < \rho \leq 2.5$ ), and high- ( $2.5 < \rho$ ) density regions.

angle. Therefore, we select  $30^\circ$  as the central angle for this study because that gives the smallest correlation coefficient. Nevertheless, as shown in Fig. 3(b), the correlation coefficient between  $\rho$  and  $v_{\text{sur}}$  is determined mainly by  $\rho$ , with the central angle being less important.

Therefore, it is inferred from this result that even when the central angle is changed, the correlation between surrounding speed and local density does not change as long as the region includes almost the same neighboring walkers. Finally, Fig. 3(c) shows the relationship between individual walking speed and surrounding speed in different local density regions. Note that the walking speeds of normal walking pedestrians are plotted. In conducting this analysis, each walker is assigned his local density, surrounding speed, and his walking speed. According to their local density, they are classified into three groups: low density, middle density, and high density. Clearly, there is a clear positive correlation between surrounding speed and walking speed, especially in the low- and middle-density regions. This means that in relatively lower density areas, people can walk freely at their desired speed while affected by their surrounding speed at the same time. On the other hand, however, in the high-density group, walking speed cannot be decided even when the surrounding speed is fixed. This tendency is clear when the surrounding speed is around 0.5 m/s. This result implies that, in high-density areas, people cannot walk at their desired speed anymore, because the walking speed is mainly determined by their local density and positions of other walkers in front of them, which determines whether the faster pedestrians can bypass slower pedestrians or not.

Consequently from Figs. 2(c) and 3(b), it is interesting to note that the density regime in which Cohen's  $d$  becomes high for both the slow mix and the fast mix (from 1.2 to  $2.4 \text{ m}^{-2}$ ) agrees well with that in which the correlation between speed and local density becomes small (from 1.0 to  $2.3 \text{ m}^{-2}$ ). This suggests a regime in the fundamental diagram in which walking speed is highly dependent on surrounding speed and cannot be determined from the local density alone. We investigate this aspect quantitatively in the next section using multiple-regression analysis.

### C. Multiple -regression analysis

Using the surrounding speed and the local density as explanatory variables, as discussed in Sec. III B, we conducted multiple-regression analysis to investigate which factor (local density or surrounding speed) affects a pedestrian's walking speed more significantly in a heterogeneous crowd.

However, before doing so, we must choose the appropriate density range in which  $\rho$  and the surrounding speed are not correlated. As discussed in Sec. III B, because we identified a region in which walking speed is apparently influenced mainly by surrounding speed, we analyze the datasets in that region.

Accordingly, the data are chosen from the local density range between 0.9 and  $2.3 \text{ m}^{-2}$ , wherein the absolute value of the correlation coefficient between these two variables is less than 0.2 (the actual value is  $-0.194$ ); this ensures that local density and surrounding speed are mutually independent in these samples. In fact, in low- ( $\rho \leq 0.9 \text{ m}^{-2}$ ) and

TABLE II. Results of multiple regression analysis.

Variable	Coefficient	$p$ value	95.0% Confidence Interval (CI)
$\bar{\rho}_l$	-0.248	Lower than $10^{-3}$	[-0.266, -0.230]
$\bar{v}_{\text{sur}}$	0.475	Lower than $10^{-3}$	[-0.457, -0.493]

high- ( $\rho \geq 2.3 \text{ m}^{-2}$ ) density regions, the correlation coefficients of the two explanatory variables are  $-0.33$  and  $-0.37$ , respectively, which implies the existence of multicollinearity in analyzing these regions. Therefore, multiple regression analyses are considered to be valid conducted only for the middle-density region (the results of other regions are shown in the Appendix).

Next, we standardized each variable by means of Eq. (3),

$$\bar{x} = \frac{x - \mu}{\sigma}, \quad (3)$$

where  $\mu$  is the mean of  $x$  and  $\sigma$  is the standard deviation of  $x$ . The normalized parameters are walking speed, local density, and surrounding speed. Thus, the coefficient of the regression analysis can be regarded as the contribution that each explanatory variable makes to the walking speed.

The regression equation is calculated as

$$\bar{v} = -0.25 \bar{\rho}_l + 0.48 \bar{v}_{\text{sur}}, \quad (4)$$

where  $\bar{v}$ ,  $\bar{\rho}_l$ , and  $\bar{v}_{\text{sur}}$  are nondimensional normalized parameters that represent walking speed, local density, and surrounding speed, respectively.

From Eq. (4), there is a negative correlation between walking speed and local density as elucidated in previous research, whereas the surrounding speed has a positive effect on walking speed. The results of this multiple-regression analysis are detailed in Table II, wherein the  $p$  value for  $v_{\text{sur}}$  is less than  $1.0 \times 10^{-3}$ , from which we conclude that the surrounding speed has a significant effect on the walking speed, as does the local density.

Although the prevailing opinion has been that local density is the most important factor in determining the walking speed of a pedestrian in a crowd, we stress that the surrounding speed should be considered when analyzing a heterogeneous-speed crowd.

It might be implied from this result that in middle-density scenarios, pedestrians control and measure their speed from visual information about the walking speed of those around them. In the fast-mix case, the implication is also that pedestrians who are walking normally are under pressure to synchronize with those around them who are walking faster and accelerate automatically.

However, the speed difference between the faster group and slower group would also contribute to how much each walker is affected by their surroundings. Although it is not confirmed in these experiments, it might be plausible that the effect of surrounding speed would be smaller if the speed difference between faster and slower groups was too large. This is because a person would not try to synchronize with other walkers if he or she notices that the surrounding people have a different desired speed which is beyond his or her

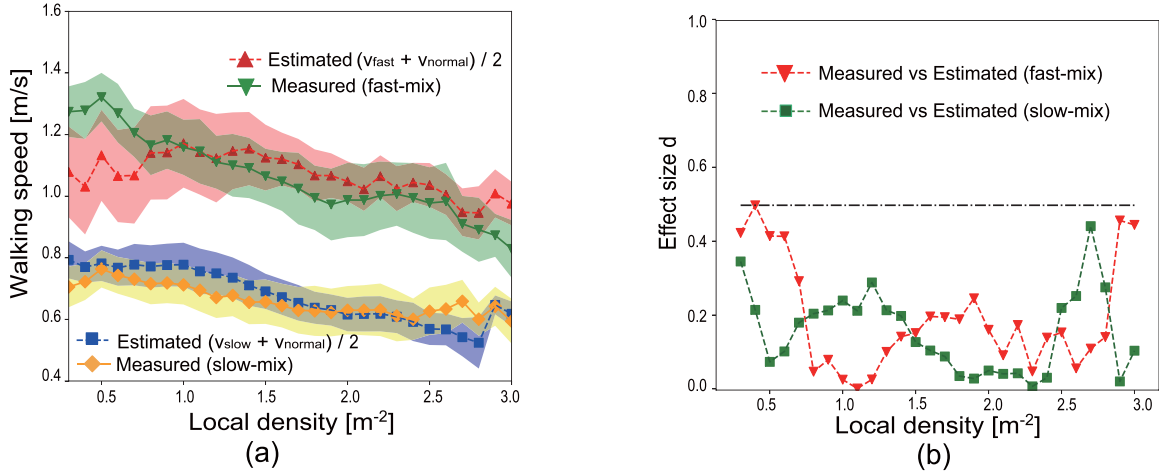


FIG. 4. (a) Estimated mean speed compared with actual mean speed. The solid lines represent the measured mean speeds of the fast-mix and slow-mix runs, and the dotted lines represent the estimated speeds of these flows, each of which is calculated as the simple mean of the two homogeneous flows. The shaded areas represent one-sigma errors for each speed. (b) The effect size *d* of the *t* test to examine whether measured speed and estimated speed are significantly different.

comfortable speed. Further research would be necessary to elucidate these effects of speed gap.

#### IV. MACROSCOPIC ANALYSIS OF HETEROGENEOUS FLOW

##### A. Decrease in mean speed in heterogeneous flow

How would we estimate the mean speed in a mixed crowd comprising *m* people who are young and *n* people who are elderly? If the global density is low enough and people can walk freely at their desired speed, then the mean speed should be the simple mean of the speed of each pedestrian. Namely, for the crowd of *m* people who are young and *n* people who

are elderly, the mean speed would be estimated as

$$v_{\text{est}} = \frac{\sum_{i \in \text{young}} v_i + \sum_{j \in \text{elderly}} v_j}{m + n}. \quad (5)$$

We discuss the validity of estimating the mean speed as Eq. (5) by comparing the estimated mean speed against the value measured experimentally, the results of which are shown in Fig. 4(a).

We wish to explain how we calculate “estimated” and “measured” speed of heterogeneous flow. For instance, the estimated speed of the fast-mix runs is calculated as  $(v_{\text{fast}} + v_{\text{normal}})/2$ , where  $v_{\text{fast}}$  is the speed of fast walkers in homogeneous flow and  $v_{\text{normal}}$  is that of normal pedestrians in homogeneous flow. In other words, the estimated speed can be regarded as the ideal speed because the actual speed is

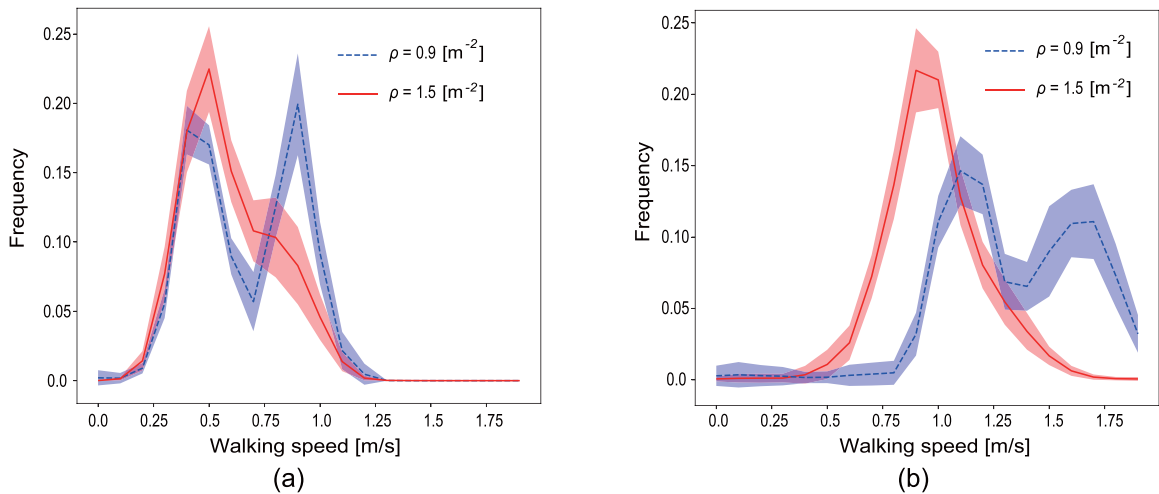


FIG. 5. Speed distribution of different runs:  $\rho_g = 0.9$  and  $1.5 \text{ m}^{-2}$  for both (a) slow-mix condition and (b) fast-mix condition. The horizontal axis represents walking speed and the vertical axis represents frequency (namely, appearance probability). The error bar represents the chronological fluctuation in frequency during one experimental run. Blue dotted lines represent experiment under  $\rho_g = 0.9$ , while red solid lines represent  $\rho_g = 1.5$ .

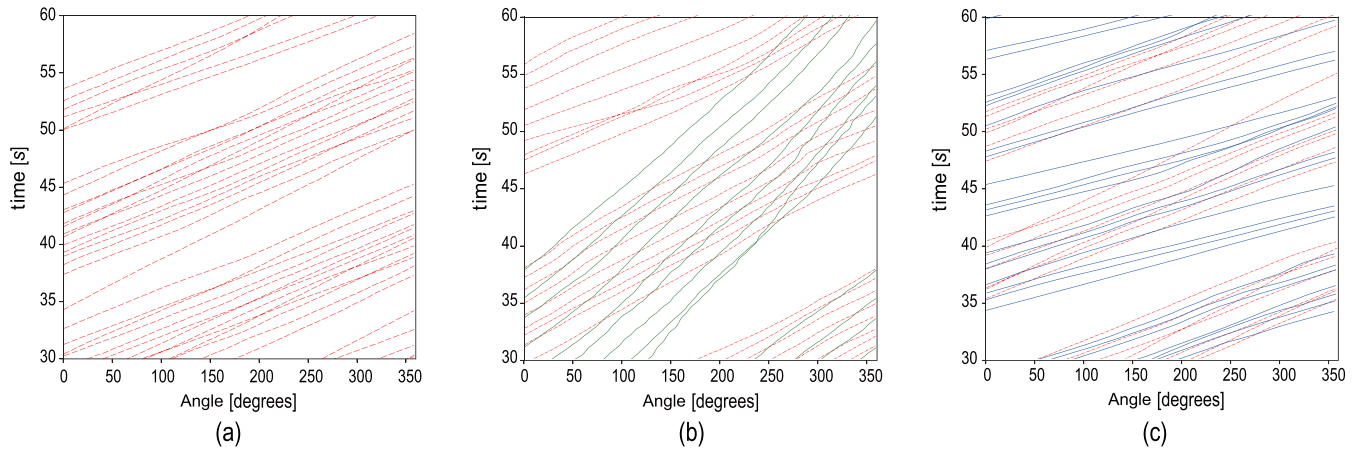


FIG. 6. Time-space diagrams for low-density ( $\rho_g = 0.7 \text{ m}^{-2}$ ) conditions. Red dotted lines represent the trajectories of normal walkers while the green and blue solid lines represent slow and fast walkers, respectively: (a) normal homogeneous runs; (b) heterogeneous slow-mix runs: red dotted lines for normal walkers and green for slow walkers; (c) heterogeneous fast-mix runs: red dotted for normal walkers and blue for fast walkers.

equal to the estimated (ideal) speed when the two groups (the slower and faster groups) walk independently of each other. A good example in which the ideal speed can be achieved is lane formation, which is known to arise spontaneously in counterflow situations [23–27].

On the other hand, as for measured speed, the walker’s speed in heterogeneous flow is averaged. For instance, when we calculate the mean speed of the fast-mix flow, the mean speeds of both normal and fast walkers in fast-mix flow are averaged. Note that only the dataset of fast-mix (heterogeneous) runs are used. Thus, we obtain the speed of the estimated and measured speed of heterogeneous velocity flow.

Interestingly, as shown in Fig. 4(a), the actual speed is generally lower than the estimated speed, which is essentially because of the blocking phenomenon whereby faster pedestrians are blocked by preceding slower pedestrians. For both slow-mix and fast-mix conditions, measured speed and the estimated speed were observed to be different. However, as

shown in Fig. 4(b), the effect size of the  $t$  test conducted to examine the difference between measured and estimated speed is not high enough to conclude the statistical difference. Further experiments should be conducted to examine this point. However, in the high-density region in the slow-mix experiments ( $\rho \geq 2.1 \text{ m}^{-2}$ ), the actual speed is higher than the estimated speed, which is considered to be because of the acceleration during bypassing behavior. In addition, even though lanes are known to form spontaneously in bidirectional flow, lane formation was not observed in these experiments.

This result supports the findings of a previous study that investigated macroscopic self-organization in a heterogeneous-speed pedestrian flow [28], where the lane formation phenomena did not occur, either. Therefore, the implication is that lane formation due to a speed difference in unidirectional flow is less likely to occur than one that occurs in bidirectional flow. The duration of each experiment and the corridor width are both thought to contribute to the presence or absence of the

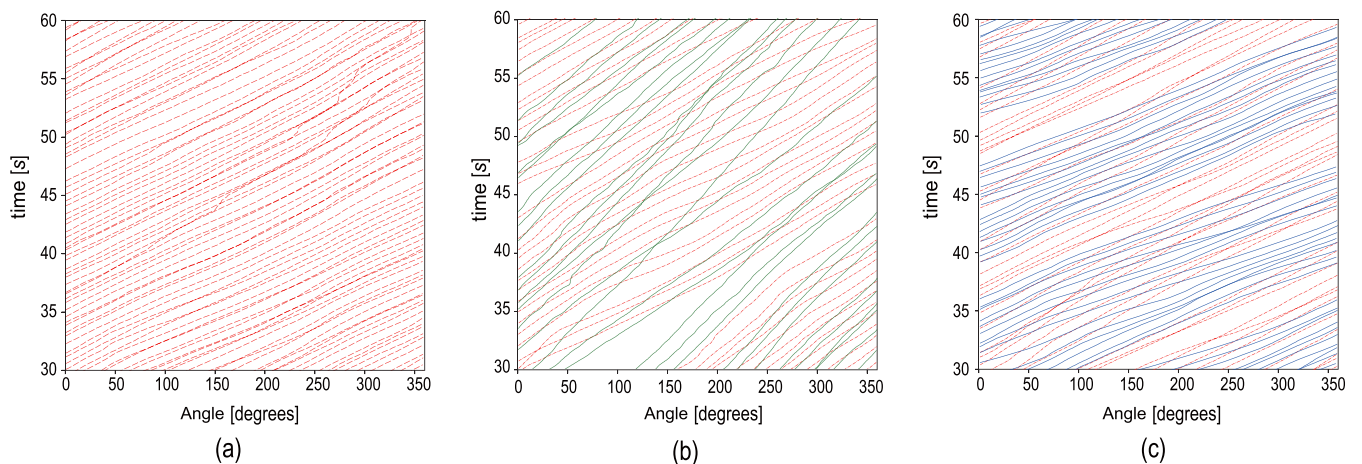


FIG. 7. Time-space diagrams for high-density ( $\rho_g = 1.5 \text{ m}^{-2}$ ) conditions: (a) normal homogeneous runs; (b) heterogeneous slow-mix runs: red dotted lines for normal walkers and green for slow walkers; (c) heterogeneous fast-mix runs: red dotted for normal walkers and blue for fast walkers.

lane formation phenomena. These points will be discussed in detail in Sec. V.

**B. Speed distribution**

To examine how freely faster walkers in each heterogeneous run are walking, we prepared speed distribution curves as shown in Fig. 5. In Fig. 5, clear double peaks are shown for lower density runs ( $\rho_g = 0.9 \text{ m}^{-2}$ ) for both slow-mix and fast-mix runs. This implies that faster pedestrians in both heterogeneous flow can walk at their desired speed in these lower density conditions. In higher density conditions, namely, when  $\rho_g = 1.5 \text{ m}^{-2}$ , there is only one single peak that is equal to the speed of slower pedestrians. In slow mix, this single peak is equal to the speed of a slower walker's desired speed, which means that faster walkers are more or less blocked by slower walkers. On the other hand, in fast-mix cases, the single peak for the case of  $\rho_g = 1.5 \text{ m}^{-2}$ , is lower than the lower peak of the distribution curve of  $\rho_g = 0.9 \text{ m}^{-2}$ .

We consider this is because of the difference in head distance between slow walkers and normal walkers. While the slow walkers can walk at their target speed in both 0.9 and  $1.5 \text{ m}^{-2}$  because they need shorter head distance compared to normal walkers, normal walkers cannot maintain their desired speed in the high-density ( $1.5 \text{ m}^{-2}$ ) conditions even in fast-mix conditions. Therefore, only the normal walkers decrease their walking speed in the high-density conditions in the slow-mix case. On the other hand, in fast-mix conditions, both the normal and the fast walkers decrease their speed. The speed distribution curves for other global densities are shown in the Appendix.

**C. Time-space diagrams**

Figures 6 and 7 show the time-space diagrams for runs at low global density ( $\rho_g = 0.7 \text{ m}^{-2}$ ) and high global density ( $\rho_g = 1.5 \text{ m}^{-2}$ ), respectively. Because the present experiments involved a circular configuration, we use the angle for detecting location and neglect the radial direction. Trajectories of walkers between 30 and 60 s from the start of experiments are plotted.

Since no congested flow was observed in this experiment, no step-and-go wave can be seen from the time-space diagrams. Instead, bypassing behaviors are clearly shown in heterogeneous runs, as in Figs. 6(b) and 6(c). In addition, the numbers of bypassing behaviors are plotted in Fig. 8. The total numbers of bypassing behavior increase as the global density increases. On the other hand, however, in slow-mix conditions, the mean numbers of bypassing behavior that each faster walker makes during one experiment does not necessarily increase with the global density, which is illustrated in high-density slow-mix runs ( $\rho_g = 1.1, 1.3, 1.5 \text{ m}^{-2}$ ). It is interesting to note that the numbers of slower walkers, whose increase in number may directly contribute to the mean numbers of bypassing behavior of a faster walker because of the increase in encounters of slower and faster walkers, does not lead to the increase in bypassing behavior. In other words, this implies that the increase in slower walkers, especially in high-density environments, is more likely to cause a drop in walking efficiency of faster walkers.

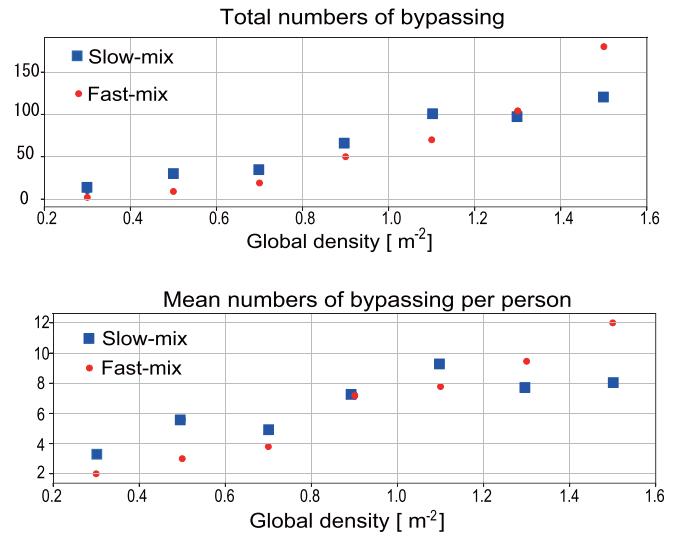


FIG. 8. Numbers of passing. For both upper and lower figures, the blue squares represent the numbers of bypassing observed in slow-mix while the red circle represent those of fast-mix conditions.

Besides, in the high-density trials, Fig. 7(a) shows small variance in spatial density distribution in the homogeneous run, while the spatial density distribution is larger especially for the high-density slow-mix run. This suggests that pedestrians were more likely to move forming clusters in the slow-mix crowd, which is triggered by a block of slower walkers preventing faster pedestrians from walking at their desired speed. This effect is thought to be more significant when there is a larger speed gap between slower and faster pedestrians. Apparently, the formation of clusters led to the density gaps, corresponding to the white regions in the time-space diagrams, which in turn led to the lower walking efficiency of pedestrians as shown in Fig. 4.

The variance in density distribution is plotted in Fig. 9, where the vertical axis represents the density variance and the horizontal axis represents the global density. This supports the assertion that the density gaps were larger in the heterogeneous runs. Thus, even though the global density was the

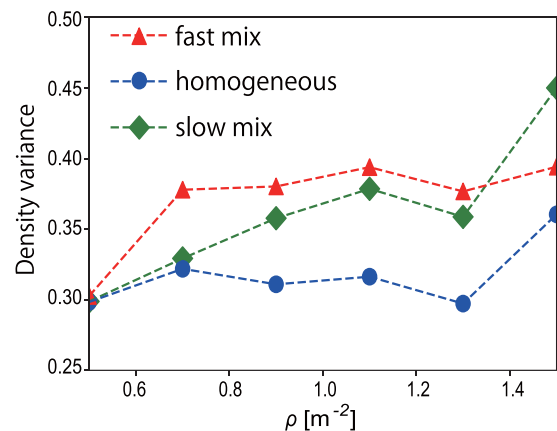


FIG. 9. Variance in density distribution. The density variance at each time is averaged through one whole run.

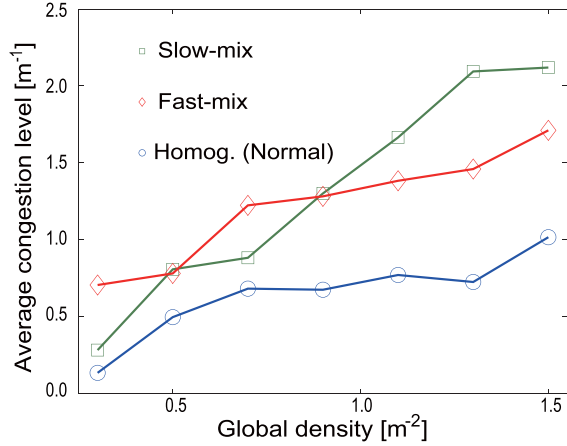


FIG. 10. Congestion levels for different crowd types depending on walking-speed composition.

same, the density distribution across the entire experimental area differed according to the composition of the flow. In heterogeneous flow, walkers form clusters when there is a “block” of slower pedestrians in front of faster pedestrians, which eventually triggers the formation of clusters and hence density gaps.

#### D. Congestion level

To further analyze the differences between homogeneous and different types of heterogeneous crowds from a physical perspective we also consider congestion level and crowd danger (details of which are provided in [29,30]), which measure different aspects of collective pedestrian dynamics.

The congestion level allows us to assess the degree of organization in a pedestrian crowd and determine the smoothness of its motion. Its definition is generally based on the rotation of the velocity vector field, although the calculation is performed in an algorithmic and more complex way (readers interested in details are referred to [29,30]). The fundamental equation defining the congestion level ( $C_l$ ) is given by

$$C_l = \frac{\max(r_z) - \min(r_z)}{|\vec{v}|}, \quad (6)$$

where  $|\vec{v}|$  is the average absolute velocity and  $r_z$  is the  $z$  component of the rotation of the velocity vector field, defined as

$$\vec{R}(x, y) = \begin{pmatrix} r_x \\ r_y \\ r_z \end{pmatrix} = \vec{\nabla} \times \vec{v}(x, y). \quad (7)$$

Low levels of congestion are associated with a synchronized, organized motion in the group, whereas high levels are typical of chaotic motion occurring, for example, during a stampede or a crowd accident. We computed the average congestion level over the entire experimental area and for all the experimental conditions considered herein, and the results are shown in Fig. 10. Because the congestion level is calculated in small time steps, the values shown here are the averages over the entire duration of each experimental run.

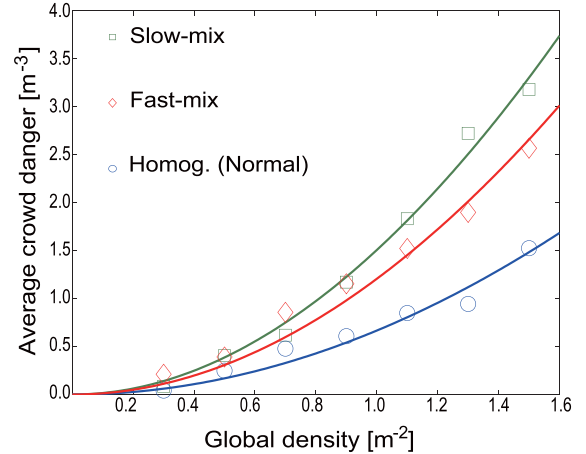


FIG. 11. Crowd danger for different types of crowds depending on walking-speed composition. Each set of points is fitted using Eq. (9).

As Fig. 10 clearly shows, the congestion level is always higher in the heterogeneous cases (for both the fast mix and the slow mix) than in the homogeneous ones. The slow mix appears to be slightly more congested, although the difference only appears for densities above  $1 \text{ m}^{-2}$ .

Next, we also consider the crowd danger, which is defined as the product of congestion level and the density, namely,

$$C_d(\rho) = \rho C_l(\rho). \quad (8)$$

Crowd danger considers how a crowd of people moves and also the density of that crowd. Consequently, congested dense crowds have very high crowd danger, whereas uncongested sparse crowds have very low crowd danger. The crowd danger for the different experiments of the present study is shown in Fig. 11.

Again, also in the case of the crowd danger, there is a clear distinction between the homogeneous and heterogeneous cases, with both heterogeneous cases having consistently higher values of crowd danger (for the same density). But to further study the properties of homogeneous and heterogeneous flows and compare them with typical cases of pedestrian motion, we would like to make use of some properties of the congestion level and the crowd danger.

In previous research we showed that congestion level and crowd danger have peculiar characteristics. The congestion level seems to have an absolute maximum value, reached in the case of chaotic motion. Also, by varying density in a constant experimental setup (as is the case for this study) we

TABLE III. Typical  $\kappa$  values for different types of pedestrian streams [29].

Type of motion	Typical $\kappa$
Unidirectional motion	$< 0.10 \text{ m}^2$
Bidirectional flow (counterflow)	$\approx 0.15 \text{ m}^2$
Multidirectional motion (crossflow, etc.)	$> 0.20 \text{ m}^2$



FIG. 12. Variance in density distribution. The density variance at each time is averaged through one whole run.

showed that crowd danger follows a typical function given by

$$C_d(\rho) = C_{I_{\max}}\rho(1 - e^{-\kappa\rho}) \quad (9)$$

with  $\kappa$  being an empirical parameter and  $C_{I_{\max}}$  being the previously mentioned maximum congestion level (approximately  $15 \text{ m}^{-2}$ ).

By fitting the different datasets of Fig. 11 with Eq. (9), we obtain  $\kappa = 0.1058 \text{ m}^2$  ( $R^2 = 0.990$ ) for the slow mix,  $\kappa = 0.0838 \text{ m}^2$  ( $R^2 = 0.967$ ) for the fast mix, and  $\kappa = 0.0455 \text{ m}^2$  ( $R^2 = 0.953$ ) for the (normal) homogeneous case. These values are typical for unidirectional configurations (see Table III for typical  $\kappa$  values of different pedestrian streams), showing that, despite the heterogeneous composition, the unidirectional nature is predominant in maintaining smooth motion.

To conclude, we showed that the heterogeneous and homogeneous cases differ in nature, and heterogeneous crowds are more likely to result in congestion and are generally more risky than homogeneous crowds of the same density. However, the exact composition of a heterogeneous crowd (i.e., slow or fast mix) seems to have little impact on either its congestion level or its intrinsic risk.

### V. CONCLUSION

In this study, the effect of speed heterogeneity on pedestrian flow was investigated in a series of experiments conducted in a circular corridor with enough space for two-dimensional behavior to occur. In these experiments, the participants were divided into three groups, a slow group, a normal group and a fast group, each of which walked at a different speed ( $0.51 \pm 0.06 \text{ m/s}$  for the slow group,  $1.09 \pm 0.05 \text{ m/s}$  for the normal group, and  $1.71 \pm 0.2 \text{ m/s}$  for the fast group). Compositions involving (i) the normal group and the fast group (the fast mix) and (ii) the normal group and the slow group (the slow mix) were tested. All the analyses in this study were based on data obtained from these experiments, with the pedestrian trajectories being extracted by PeTrack.

The fundamental diagrams show that local density is not the only factor that determines the speed at which a person walks, and the speed of those walking nearby also has an effect. Moreover, by conducting multiple-regression analysis, we find quantitatively that the surrounding speed is more important than the local density in determining the walking speed, especially in the quasifree regime. Consequently, this study implies that the surrounding speed should be taken into account in addition to the local density, even though most previous studies did not consider the former. In that sense, the present study succeeded in finding an important factor with which to investigate heterogeneous crowds.

As for the macroscopic flow characteristics, the mean speed became lower than the simple mean speed of the crowd constituents when the two flows mixed. In other words, the spontaneous lane formation that is known to occur in bidirectional flow does not occur in heterogeneous-speed flow.

Several elements are thought to contribute to the absence of lane formation in our experiments: the duration of each experiment, corridor width, walking direction, and density. In our experiments, walkers did not “learn” to walk separately, which we consider as the crucial reason for the absence of lane formation. In fact, there is a relevant bidirectional experiment with a similar setup as the present experiment [29]. Although lanes were formed in most of the runs in [29], the first run was

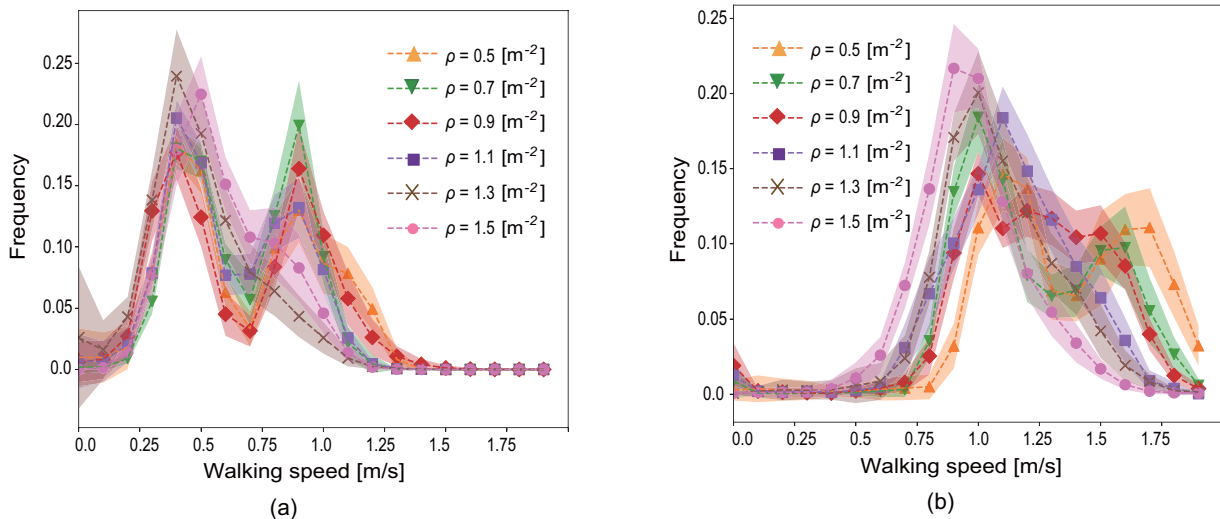


FIG. 13. Speed distribution of different runs:  $0.5 \leq \rho_g \leq 1.5$  for both (a) slow-mix condition and (b) fast-mix condition.

the only exception where lanes were not formed. The reason for the absence of lanes is concluded that walkers had not “learned to” walk separately. Accordingly, it is also inferred from the bidirectional experiment that the experiment duration is important at least when walkers have not experienced lane formation.

Besides, in bidirectional flow, if a pedestrian do not give way to pedestrians coming from the opposite direction, not only counterwalking pedestrians but also the given pedestrian’s walking efficiency drops largely because of collision. This would give each walker the motive to walk separately, which consequently leads to lane formation. In our experiments, however, the situations where slower walkers give way to faster walkers coming behind them were not observed, because their walking efficiency would not drop even if they do not give way to faster walkers coming behind them.

As for the effect of density, since the pedestrians in the present study did not “learn” to create lanes, the existence of lanes is thought to be stochastic. Therefore, the probability of lane formation would be higher in lower density scenarios, where each group of pedestrians is allowed to walk at their target speed. Nevertheless, further research is necessary to investigate the effect of density on lane formation phenomena. Because of these argumentations, we wish to conclude that in unidirectional flow with different desired speed, the lane formation phenomena would be more unlikely to occur compared to bidirectional flow.

Accordingly, it would be highly advisable to introduce sidewalk markings or lane dividers in pedestrian walkways to promote lane formation. The analysis using time-space diagrams shows that there is a huge gap in the density distribution map in front of the head of the cluster, especially under slow-mix conditions. The speed distribution reveals the threshold by which faster pedestrians can no longer walk at their desired speed. At the same time, congestion level and crowd danger, both of which estimate intrinsic risk in crowd movements, are always higher in a heterogeneous-speed crowd. Thus, we conclude that heterogeneous and homogeneous flows are essentially different, and we also wish to emphasize that lane dividers to promote heterogeneous flow might mitigate the rising levels of congestion in cities.

As further research, various aspects are of importance and relevance to the present study. Regarding heterogeneous-speed pedestrian flows, the rush ratio, which is the ratio of slower and faster pedestrians, could also be varied. A relatively low rush ratio means that the flow can be regarded as almost homogeneous, meaning that there might be a phase transition that would change the flow characteristics drastically. Moreover, even though the jamming state was not observed in the present study and all the experiments were conducted in the free-flow regime, different physics and phenomena might appear under different flow conditions.

#### ACKNOWLEDGMENTS

This work was supported by JST-Mirai Program Grant No. JPMJMI17D4, Japan, JSPS KAKENHI Grant No. JP15K17583, and MEXT as “Post-K Computer Exploratory Challenges” (Exploratory Challenge 2: Construction of Models for Interaction Among Multiple Socioeconomic

TABLE IV. Results of multiple regression analysis in low-density regions.

Variable	Coefficient	$p$ value	95.0% CI
$\bar{\rho}_l$	-0.207	0.010	[-0.126, -0.289]
$\bar{v}_{\text{sur}}$	0.622	Lower than $10^{-3}$	[0.631, 0.794]

Phenomena, Model Development and its Applications for Enabling Robust and Optimized Social Transportation Systems) (Project ID: hp180188). The experiments were organized with the help of members of the Nishinari laboratory. We are particularly grateful to Takahiro Ezaki and Hisashi Murakami for their support.

#### APPENDIX

##### 1. Measurement of each group’s desired speed

We measured the mean desired speed of each group (slow, normal, and fast walkers) as follows. For slow and normal groups, low-density homogeneous experiments ( $\rho_g = 0.1, 0.3, 0.5$ ) were used to measure their desired speed, since they are unlikely to be affected by local density in this density. Accordingly, 18 people’s speeds were measured as the desired speed of slow and normal groups. On the other hand, for fast walkers, they were told to walk the corridor alone (shown in Fig. 12), and we measured the time that each walker spent on walking the corridor. The reason why we measured the fast walkers differently is that fast walkers are thought to be sensitive to local density, while slow and normal walkers are not, at least in low-density regions.

##### 2. Speed distribution

In Sec. IV, the speed distribution of only two experiments ( $\rho_g = 0.9, 1.5$ ) are shown for both slow-mix and fast-mix cases. The speed distribution of runs under other  $\rho_g$  are shown in Fig. 13. We see from Fig. 13(a) that the peak at 0.9 m/s, which represents the speed of normal walkers’ desired speed, disappears when the global density is more than  $1.1 \text{ m}^{-2}$ . Similarly, from Fig. 13(b) the peak at 1.6 m/s, namely, the speed of fast walkers, cannot be seen when the global density is more than  $0.9 \text{ m}^{-2}$ . For further analysis, an experiment with detailed increments of global density would be necessary.

##### 3. Multiple regression analysis on other regions

The results of the multiple regression analysis in low- and high-density regions are shown in Tables IV and V. However, there is a chance that the analyses in these density regions contain multicollinearity.

TABLE V. Results of multiple regression analysis in high-density regions.

Variable	Coefficient	$p$ value	95.0% CI
$\bar{\rho}_l$	-0.108	0.131	[-0.391, -0.055]
$\bar{v}_{\text{sur}}$	0.462	0.131	[0.239, 0.685]

- [1] D. Helbing and P. Mukerji, Crowd disasters as systemic failures: Analysis of the love parade disaster, *EPJ Data Sci.* **1**, 7 (2012).
- [2] B. Krausz and C. Bauckhage, Loveparade 2010: Automatic video analysis of a crowd disaster, *Comput. Vis. Image Und.* **116**, 307 (2012).
- [3] D. Helbing, I. Farkas, and T. Vicsek, Simulating dynamical features of escape panic, *Nature (London)* **407**, 487 (2000).
- [4] A. Seyfried, B. Steffen, W. Klingsch, and M. Boltes, The fundamental diagram of pedestrian movement revisited, *J. Stat. Mech.: Theory Exp.* (2005) P10002.
- [5] A. Seyfried, M. Boltes, J. Kähler, W. Klingsch, A. Portz, T. Rupperecht, A. Schadschneider, B. Steffen, and A. Winkens, Enhanced empirical data for the fundamental diagram and the flow through bottlenecks, *Pedestrian and Evacuation Dynamics 2008* (Springer, New York, 2010), pp. 145–156.
- [6] J. Zhang, W. Klingsch, A. Schadschneider, and A. Seyfried, Transitions in pedestrian fundamental diagrams of straight corridors and T-junctions, *J. Stat. Mech.: Theory Exp.* (2011) P06004.
- [7] M. Boltes, J. Zhang, A. Seyfried, and B. Steffen, T-junction: Experiments, trajectory collection, and analysis, in *2011 IEEE International Conference on Computer Vision Workshops (ICCV Workshops)* (IEEE, New York, 2011), pp. 158–165.
- [8] D. Yanagisawa, A. Tomoeda, and K. Nishinari, Improvement of pedestrian flow by slow rhythm, *Phys. Rev. E* **85**, 016111 (2012).
- [9] U. Chattaraj, A. Seyfried, and P. Chakroborty, Comparison of pedestrian fundamental diagram across cultures, *Adv. Complex Syst.* **12**, 393 (2009).
- [10] U. Chattaraj, A. Seyfried, P. Chakroborty, and M. K. Biswal, Modelling single file pedestrian motion across cultures, *Procedia-Soc. Behav. Sci.* **104**, 698 (2013).
- [11] C. Thornton, R. O’Konski, B. Hardeman, and D. Swenson, Pathfinder: An agent-based egress simulator, *Pedestrian and Evacuation Dynamics* (Springer, New York, 2011), pp. 889–892.
- [12] A. Gorrini, G. Vizzari, and S. Bandini, Age and group-driven pedestrian behaviour: From observations to simulations, *Collect. Dyn.* **1**, 1 (2016).
- [13] C. Feliciani and K. Nishinari, Phenomenological description of deadlock formation in pedestrian bidirectional flow based on empirical observation, *J. Stat. Mech.: Theory Exp.* (2015) P10003.
- [14] T.-Q. Tang, L. Chen, R.-Y. Guo, and H.-Y. Shang, An evacuation model accounting for elementary students individual properties, *Physica A* **440**, 49 (2015).
- [15] H. Klüpfel, T. Meyer-König, and M. Schreckenberg, Comparison of an evacuation exercise in a primary school to simulation results, in *Traffic and Granular Flow’01* (Springer, New York, 2003), pp. 549–554.
- [16] M. Spearpoint and H. A. MacLennan, The effect of an ageing and less fit population on the ability of people to egress buildings, *Safety Sci.* **50**, 1675 (2012).
- [17] M. Manley, Y. S. Kim, K. Christensen, and A. Chen, Modeling emergency evacuation of individuals with disabilities in a densely populated airport, *Transp. Res. Rec.* **2206**, 32 (2011).
- [18] J. Koo, Y. S. Kim, and B.-I. Kim, Estimating the impact of residents with disabilities on the evacuation in a high-rise building: A simulation study, *Simul. Model. Pract. Theory* **24**, 71 (2012).
- [19] J. Koo, Y. S. Kim, B.-I. Kim, and K. M. Christensen, A comparative study of evacuation strategies for people with disabilities in high-rise building evacuation, *Expert Syst. Appl.* **40**, 408 (2013).
- [20] S. Cao, J. Zhang, D. Salden, J. Ma, C. Shi, and R. Zhang, Pedestrian dynamics in single-file movement of crowd with different age compositions, *Phys. Rev. E* **94**, 012312 (2016).
- [21] A. Fujita, C. Feliciani, D. Yanagisawa, and K. Nishinari, Traffic flow in a crowd of pedestrians walking at different speeds—dataset, <http://ped.fz-juelich.de/extda/fujita2017>, accessed 1 April 2019.
- [22] D. E. Farrar and R. R. Glauber, Multicollinearity in regression analysis: The problem revisited, *Rev. Econ. Stat.* **49**, 92 (1967).
- [23] D. Helbing, L. Buzna, A. Johansson, and T. Werner, Self-organized pedestrian crowd dynamics: Experiments, simulations, and design solutions, *Transp. Sci.* **39**, 1 (2005).
- [24] M. Isobe, T. Adachi, and T. Nagatani, Experiment and simulation of pedestrian counter flow, *Physica A* **336**, 638 (2004).
- [25] Y. Suma, D. Yanagisawa, and K. Nishinari, Anticipation effect in pedestrian dynamics: Modeling and experiments, *Physica A* **391**, 248 (2012).
- [26] C. Feliciani and K. Nishinari, An improved cellular automata model to simulate the behavior of high density crowd and validation by experimental data, *Physica A* **451**, 135 (2016).
- [27] J. Zhang, W. Klingsch, A. Schadschneider, and A. Seyfried, Ordering in bidirectional pedestrian flows and its influence on the fundamental diagram, *J. Stat. Mech.: Theory Exp.* (2012) P02002.
- [28] M. Moussaid, E. G. Guilloit, M. Moreau, J. Fehrenbach, O. Chabiron, S. Lemercier, J. Pettré, C. Appert-Rolland, P. Degond, and G. Theraulaz, Traffic instabilities in self-organized pedestrian crowds, *PLoS Comput. Biol.* **8**, e1002442 (2012).
- [29] C. Feliciani and K. Nishinari, Measurement of congestion and intrinsic risk in pedestrian crowds, *Transp. Res. C: Emerg. Technol.* **91**, 124 (2018).
- [30] C. Feliciani, H. Murakami, and K. Nishinari, A universal function for capacity of bidirectional pedestrian streams: Filling the gaps in the literature, *PLoS One* **13**, e0208496 (2018).